PNAS RESEARCH ARTICLE | BIOCHEMISTRY

Binding mode–guided development of high-performance antibodies targeting site-specific posttranslational modifications

Mariapia Riso[a], Rohan N. Shah[b,c], Akiko Koide[a,d], Alexander J. Ruthenburg[c,e], Shohei Koide[a,f], and Takamitsu Hattori[a,f,1]

Affiliations are included on p. 8.

Edited by Arne Skerra, Technische Universitaet Muenchen, Freising, Germany; received June 19, 2024; accepted November 13, 2024 by Editorial Board Member Karolin Luger

Posttranslational modifications (PTMs) of proteins play critical roles in regulating many cellular events. Antibodies targeting site-specific PTMs are essential tools for detecting and enriching PTMs at sites of interest. However, fundamental difficulties in molecular recognition of both PTM and surrounding peptide sequence have hindered the efficient generation of highly sequence-specific anti-PTM antibodies. Furthermore, the widespread use of potentially inconsistent, nonrenewable, and molecularly undefined antibodies presents experimental challenges thought to contribute to the reproducibility problem in biomedical research. In this study, we describe the binding mode-guided development of a platform that efficiently generates potent and selective recombinant antibodies to PTMs that are molecularly defined and renewable. Our platform is built on our previous discovery of an unconventional binding mode of anti-PTM antibodies, antigen clasping, where two antigen binding sites cooperatively sandwich a single antigen, creating extensive interactions with the antigen and leading to high selectivity and potency. We designed the platform that generates clasping antibodies with two distinct binding units, resulting in efficient generation of antibodies to a set of trimethylated histone H3 with high levels of specificity and affinity. Performance comparison in chromatin immunoprecipitation, a common application in epigenomics, revealed that a clasping antibody to trimethylated histone H3 at lysine 27 exhibited superior specificity to a widely used conventional antibody and captured symmetric and asymmetric nucleosomes in a less biased manner. We further generated clasping antibodies to phosphotyrosine antigens by using the same principle. These results suggest the broad applicability of our platform to generating high-performance clasping antibodies to diverse PTMs.

protein engineering | affinity reagents | epigenetics | histone modifications | signaling

Significance

Posttranslational modifications (PTMs) occur at specific sites within proteins, and each combination of PTM types and modification sites is associated with distinct roles in cellular processes. Highly specific anti-PTM antibodies are indispensable reagents for analyzing PTMs, but difficulties in selectively recognizing both PTMs and modification sites pose a significant challenge in generating such antibodies. Here, we report an efficient generation of high-performance antibodies to site-specific PTMs by a binding mode-guided approach. Our approach exploited a sandwiching binding mode of our previous highly specific anti-PTM antibodies, which creates a large antigen-binding surface, overcoming challenges in molecular recognition of site-specific PTMs. This work expands the antibody generation strategy for challenging antigens, enabling the creation of rigorous tools for the study of PTMs.

Posttranslational modifications (PTMs), such as methylation, phosphorylation, acetylation, ubiquitination, and glycosylation of proteins play crucial roles in many biological events (1–4), and dysregulation of PTMs in the context of specific protein sequences are observed in diseases, including cancer (5–8). Accordingly, the identification and quantification of site-specific PTMs are important for the analyses of PTMs. Antibodies to PTMs that recognize both PTM and sequences surrounding the modification are an essential component for enriching and detecting PTMs. However, it has been widely recognized that many available anti-PTM antibodies, which are commonly generated by animal immunization, have shortcomings (9–13).

There are two common problems with available antibodies to PTMs. First, many anti-PTM antibodies exhibit low specificity and/or low affinity, leading to cross-reactivity to off-targets or no binding to the intended target (9–13). Second, there is a large lot-to-lot variation of polyclonal antibodies generated by animal immunization. Each polyclonal antibody product is a heterogeneous mixture of antibodies derived from multiple B cells. Thus, each lot (i.e., each immunization product) of a polyclonal antibody is a distinct reagent. Monoclonal antibodies derived from a single B cell should lead to a homogenous antibody (14). Still, hybridoma cells can express multiple different antibody genes or lose the relevant antibody gene over many passages, leading to lot-to-lot variability (15, 16). Recombinant antibodies are produced by a defined expression vector, and their amino acid sequences are determined during the characterization process. Their renewability can fundamentally eliminate a major obstacle to reproducibility (12, 17). Indeed, the number of available recombinant antibodies, converted from monoclonal antibodies by cloning genes from hybridoma cells, has increased in the past decade. However, converting suboptimal monoclonal antibodies into recombinant antibodies itself does not solve the fundamental problem of low-quality anti-PTM antibodies.

This article is a PNAS Direct Submission A.S. is a guest editor invited by the Editorial Board.

[1]To whom correspondence may be addressed. Email: Takamitsu.Hattori@nyulangone.org.

This article contains supporting information online at https://www.pnas.org/lookup/suppl/doi:10.1073/pnas.2411720121/-/DCSupplemental.

Published December 30, 2024.

The challenge in generating highly selective antibodies to site-specific PTMs stems from the fundamental, biophysical difficulties in recognizing PTMs. The chemical moieties of PTMs are usually minute, and differences among PTMs (e.g., mono-, di-, and trimethylation) are subtle. In addition to specifically recognizing the target PTM, antibodies need to discriminate closely related sequences surrounding the modification. Furthermore, the PTM sites are usually located in the flexible or disordered regions on proteins (18–20), and thus, unfavorable entropic loss of a flexible peptide segment upon antibody binding hinders achieving high affinity. We previously attempted to generate site-specific anti-PTM antibodies via a standard approach combining library sorting and directed evolution. Although we were ultimately successful in generating recombinant antibodies to trimethylated histone H3 at lysine 4 (H3K4me3) and lysine 9 (H3K9me3) with high affinity and exquisite specificity (12, 21), extensive engineering and iterative optimization were required to achieve the desired outcomes. Consequently, fundamental challenges in molecular recognition hamper identifying high-performance anti-PTM antibodies regardless of the existing antibody-generation methods.

We previously discovered that our high-performance antibodies to H3K4me3 and H3K9me3 utilize an unusual binding mode, which we named "antigen clasping." Antibody fragments such as an antigen-binding fragment (Fab) or a variable fragment (Fv) contain a single antigen-binding site, and the 1:1 stoichiometry of the antibody–antigen recognition is a highly conserved recognition mode among numerous known antibodies. Unexpectedly, in our high-performance antibodies, two antigen-binding sites cooperatively sandwich one single antigen by forming a head-to-head homodimer (21). Compared with the conventional, 1:1 antibody–antigen recognition, this antigen clasping doubles the size of the antigen recognition interface, contributing to high affinity and exquisite specificity to both PTM and peptide sequence. Thus, antigen clasping is a suited binding mode for the specific recognition of PTMs in a sequence-specific manner compared to the conventional binding mode of antibodies.

Antigen clasping serendipitously emerged during the iterative optimization process. Indeed, other anti-histone methylation antibodies developed with the same approach by us exhibit no antigen clasping (12, 21). Although the emergence of antigen clasping demonstrates the power of directed evolution, the development process required multiple rounds of mutagenesis and screening. The binding mode of antigen clasping is conceptually similar to that of previously developed molecules by some of us, termed affinity clamps, where the clamshell architecture was intentionally designed (22–24). An affinity clamp consists of a naturally occurring modular binding domain, such as PDZ and Src homology 2 (SH2) domains, and a monobody that is engineered to recognize the target peptide presented by the modular binding domain (22–24). This concept has successfully been applied to peptides harboring phospho-tyrosine or the C-terminal carboxyl group (22, 24). However, the inherent peptide motif specificity of the natural domains limits the applications of affinity clamps to a broad range of peptides. In addition, the development of affinity clamps often requires extensive modifications of a modular binding domain, e.g., circular permutation (22), which may not be tolerated by a domain of interest. Nevertheless, the successes of affinity clamps and the resemblance between affinity clamps and clasping antibodies inspired us to develop clasping antibodies in an intentional, binding mode-guided approach.

Here, we report the development of a platform that efficiently generates high-performance clasping antibodies to a diverse set of trimethylated sites in histone H3 without extensive optimization steps. We further generated clasping antibodies to phospho-tyrosine antigens by the same approach, suggesting the broad applicability of our platform to producing next-generation antibodies to a variety of PTMs with diverse sequence space.

Results

Binding Mode–Guided Design of Heterodimeric Clasping Antibodies. The clasping antibodies that we previously identified are homodimers consisting of two identical Fabs (Fig. 1 *A* and *B*) (21). When these clasping antibodies bind to a histone peptide containing trimethylated Lys, an antigen that has no internal symmetry, each of the two identical Fab units plays a distinct role: one unit mainly interacts with the PTM and the other interacts with the remaining part of the peptide. The 2:1 clasping complex is also stabilized by contacts between the two Fab units (21). Because the target peptide is asymmetrical and the two Fab units play distinct roles in clasping antibodies, we designed heterodimeric clasping antibodies with two different antigen binding units, the PTM and enhancer units (Fig. 1*B*), by adopting the design of affinity clamps, where the natural peptide-binding domain and monobody are designed to be the primary and enhancer units (22–24). In our new design, the PTM unit primarily recognizes the PTM and the enhancer unit recognizes both the remaining part of the peptide and the PTM unit, achieving the antigen clasping. The enhancer unit aids in improving the sequence specificity and affinity to the intended PTM-containing peptide.

Clasping antibodies differ from bispecific antibodies in their binding mode and development process. Bispecific antibodies are composed of two distinct antigen-binding units in which each of the units recognizes different types of antigens (25). Those two binding units are developed independently, and their optimal combination is usually identified through a trial-and-error process. In contrast, although clasping antibodies are also composed of two binding units, they recognize the single antigen with overlapped epitopes in a cooperative manner. Our approach produces clasping antibodies in a streamlined process, which is composed of the identification of a PTM unit exhibiting high PTM specificity but low affinity and low sequence specificity, followed by the development of an enhancer unit via antibody library screening (see below for the details).

As a critical test of our approach, we chose a series of trimethylated histone targets (*SI Appendix*, Fig. S1*A*), because our previous directed-evolution approach generated antibodies to H3K4me3 and H3K9me3 but not to the rest (12, 21). Histone methylations are associated with important biological processes such as transcriptional activation and repression (26, 27). The abnormal activities of lysine methyltransferases and demethylases are closely linked with cancer development, leading to an elevation or loss of histone methylation (28–32). Consequently, highly specific antibodies are needed for accurate and sensitive detection of both the modification site and the methylation state for elucidating the mechanism of cancer, molecular diagnosis, and drug discovery.

We chose a previously reported antibody, 4-5, as a PTM unit, as it is highly specific to trimethylated Lys but has low affinity and low sequence specificity (12). To identify enhancer antibodies, we sorted a synthetic antibody phage-display library against the 4-5 Fab in complex with the Kme3-containing histone peptides. We used saturating amounts of peptides to ensure that the majority of the 4-5 Fab molecules form the complex with the peptides. After four rounds of selection, we identified antibody clones specifically bound to the 4-5 Fab-H3K56me3 peptide complex. To test whether these antibodies function via antigen clasping, we produced biotinylated Fabs (*SI Appendix*, Fig. S1 *B* and *C*) and

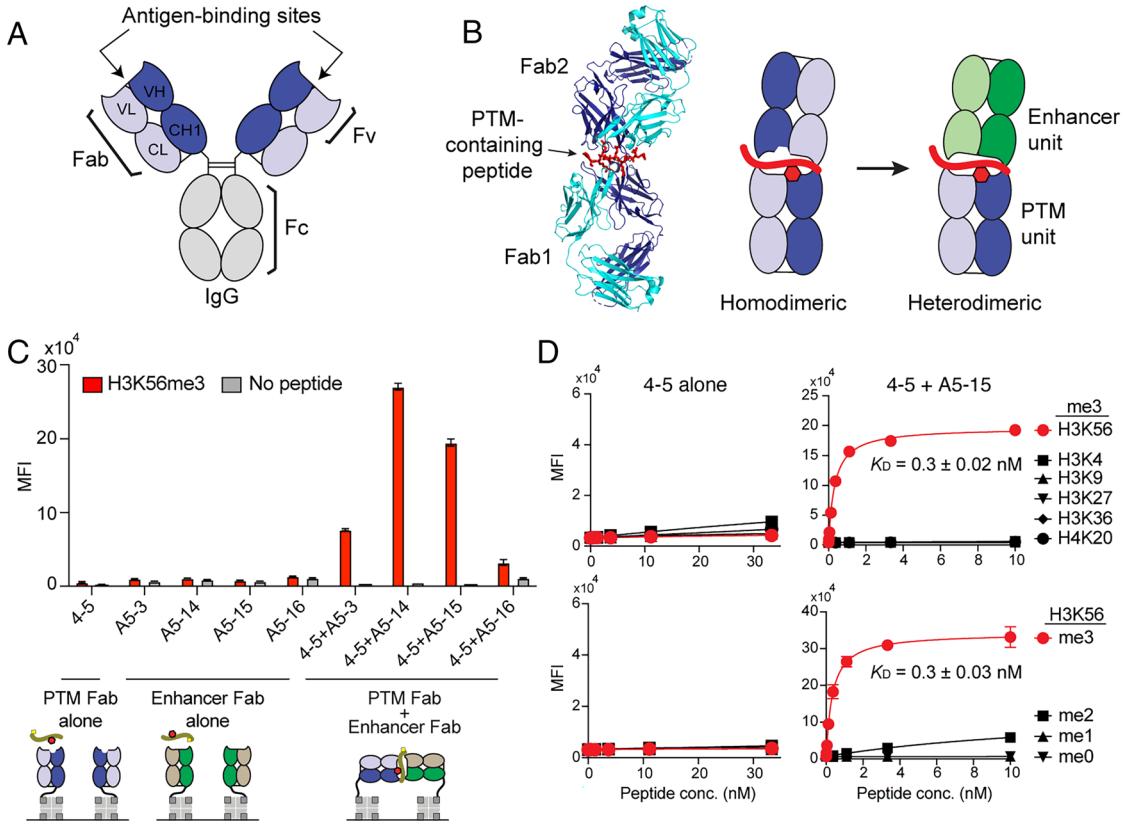

Fig. 1. Binding mode-guided design of heterodimeric clasping antibodies. (*A*) Schematic representation of IgG antibody. (*B*) The structure of homodimeric clasping antibody (PDB ID: 4YHP, *Left*) and its schematic representation (*Middle* cartoon). The *Right* cartoon represents heterodimeric antigen clasping that is composed of two different antigen-binding units, PTM and enhancer units, resembling the distinct roles of Fabs in homodimeric antigen clasping. (*C*) Binding analysis of PTM and enhancer Fabs to the H3K56me3 peptide with the peptide-IP assay. The peptide concentration used here was 100 nM. The peptide binding was observed only when both PTM and enhancer Fabs were coimmobilized on beads, indicating cooperative binding of both Fabs in an antigen-clasping manner. (*D*) Binding titration curves of PTM Fab alone and coimmobilized Fabs with the peptide IP assay. The apparent K_D values, calculated from the curve fitting of a 1:1 binding model, to the target peptide are shown. Sequence specificity (*Top*) and methylation-state specificity (*Bottom*) are assessed. Data shown here are from triplicate measurements. Error bars indicate the SD.

coimmobilized both 4-5 and enhancer Fabs on the streptavidin-coated beads, which should facilitate antigen clasping. Strikingly, the peptide IP assay (11) revealed the beads with coimmobilized Fabs showed binding to the H3K56me3 peptide, whereas beads with only one of the two Fabs did not, indicating that 4-5 and enhancer Fabs cooperatively recognize the peptide, consistent with antigen clasping (Fig. 1*C*). Notably, all coimmobilized Fabs exhibited apparent dissociation constant (K_D) values in the nanomolar to sub-nanomolar range and low cross-reactivity to off-target peptides, indicating high affinity and exquisite specificity (Fig. 1*D* and *SI Appendix*, Fig. S1 *D* and *E*). Coimmobilized Fabs did not show efficient binding to the peptides containing Kme3 with mismatched sequences (i.e., off-target Kme3 peptides) and to the peptides containing the same H3K56 sequence with mismatched PTMs (i.e., non-, mono, and dimethylated H3K56 peptides). These results indicate that the precise placement of the Kme3 modification at the specific position in the context of the sequence is essential for efficient peptide recognition by those antibodies, further supporting the clasping mechanism. Together, these data demonstrated that our streamlined approach generated heterodimeric clasping antibodies to particularly challenging PTM antigens without iterative directed evolution processes.

Improving the Throughput of Clasping Antibody Identification. To further enhance the efficiency of identifying heterodimeric clasping antibodies, we next set out to develop a yeast-display system where the enhancer single-chain variable fragment (scFv) unit is tethered to the PTM scFv unit with a long linker to facilitate intra-molecular dimerization (Fig. 2*A*). We first examined this design using the clasping antibodies against H3K56me3 with multiple long linkers (17-, 22-, and 27- amino acid linkers) between the PTM and enhancer units. Remarkably, all constructs exhibited high specificity and affinity, consistent with their binding profiles observed in the Fab format (Fig. 2*B* and *SI Appendix*, Fig. S2 *A–C*), indicating the successful antigen clasping on the yeast surface. The difference in linker length did not substantially affect the affinity of the clones, suggesting that the 17-residue linker is long enough for facilitating antigen clasping. We observed a minor difference in the binding intensity in each linker length, especially for the A5-15 and A5-16 clasping antibodies, presumably due to the difference in the expression level of these designs on the yeast surface or the difference in the binding mode of these clones compared to the others (*SI Appendix*, Fig. S2*B*). We thus chose the 22-residue linker that showed the highest binding intensity among the linker designs for both A5-15 and A5-16.

We next constructed yeast-display antibody libraries using the genes isolated from the enriched phage pools described above. Strikingly, with a few rounds of library sorting, we identified clasping antibodies exhibiting apparent K_D values in the single to sub-nanomolar range and high specificity against multiple trimethylated histone targets, including H3K9me3, H3K27me3, and H4K20me3 (Fig. 2*B* and *SI Appendix*, Fig. S3 *A–D*). We did not identify clasping antibodies to those targets by screening with phage ELISA after phage library sorting, illustrating the improved efficiency of clasping antibody identification by the secondary screening using yeast display. Given that 4-5 scFv, the PTM unit

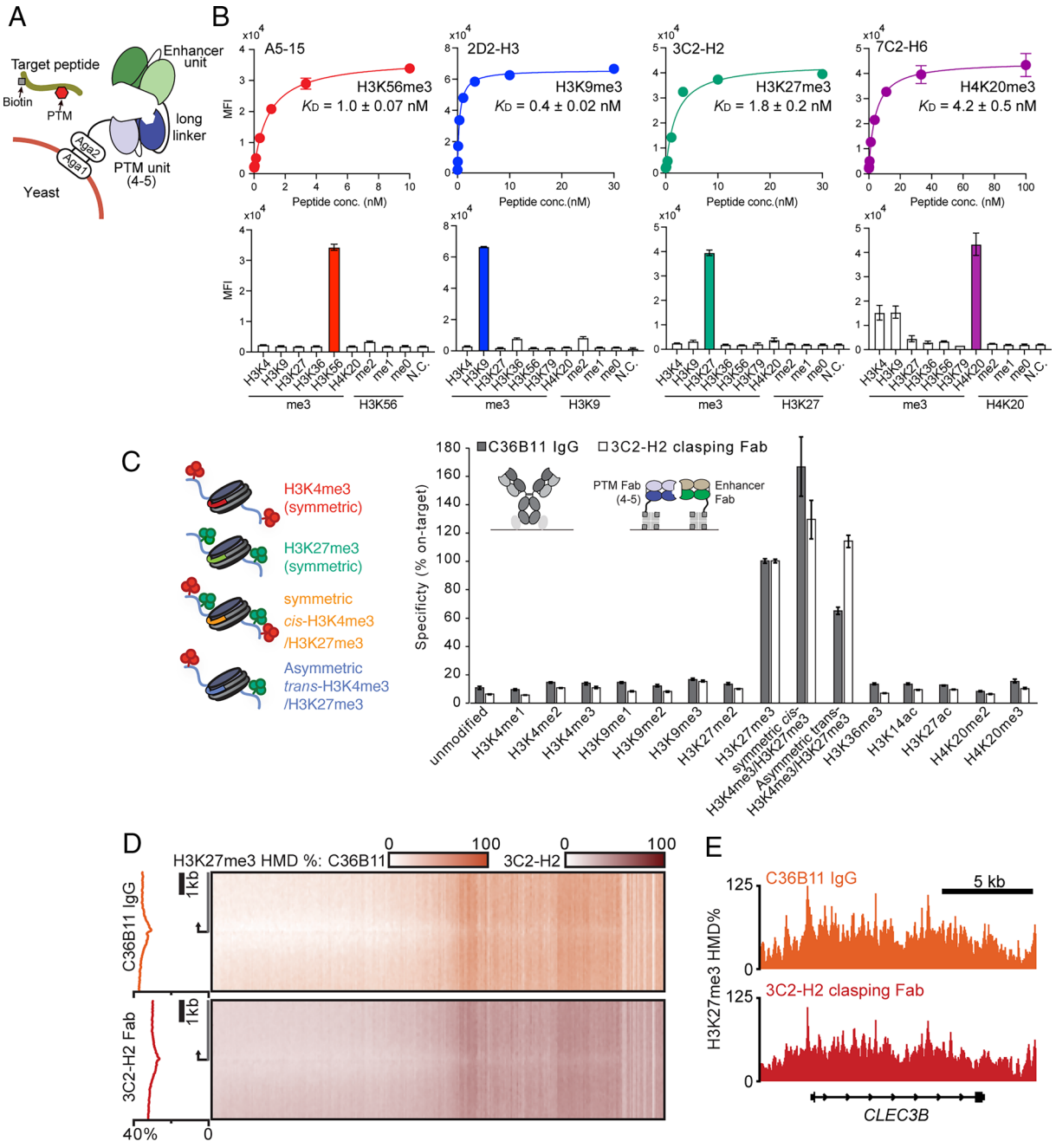

Fig. 2. Efficient identification of clasping antibodies by yeast display and characterization of anti-H3K27me3 antibody in ICeChIP. (*A*) Schematic representation of the yeast-display format where the enhancer unit is tethered to the PTM unit with a long linker. (*B*) Characterization of clasping antibodies with the peptide IP assay in the yeast-display format harboring the 22-residue linker. Binding titration curves using the target peptides (*Top*) and specificity test using off-target peptides (*Bottom*) are shown. The apparent K_D values were calculated from the curve fitting of a 1:1 binding model. The highest peptide concentrations used in the binding titration curves were utilized in the specificity test (*Bottom*). Data shown here are from triplicate measurements. Error bars indicate the SD. See also *SI Appendix*, Figs. S2 and S3 for other clones. (*C–E*) Performance comparison of the widely used antibody and the clasping antibody to H3K27me3 in native ICeChIP. (*C*) Specificity of antibodies assessed by ICeChIP. The *Left* cartoons represent the nucleosome standards bearing H3K4me3, H3K27me3, or both. Note that the different standards bearing the H3K27me3 have one or two instances of the mark per nucleosome. Antibody specificity was calculated as the percentage of off-target to on-target (H3K27me3) enrichment of nucleosome standards. The 3C2-H2 clasping antibody captured symmetric and asymmetric nucleosome standards in a less biased manner compared with C36B11 IgG. (*D*) Metagene and heatmap performance comparison of antibodies. Histone modification density (HMD) of H3K27me3 across all promoters in mESCs rank-ordered by their RNA-expression level (RNA-seq from ENCODE) was plotted. (*E*) Representative locus showing apparent H3K27me3 HMD with antibodies.

alone, exhibits apparent K_D values to the histone trimethylated peptides in the micromolar range (12), the apparent K_D values of these clasping antibodies correspond to >1,000-fold increases in affinity to their respective targets. Our clasping antibodies to H3K9me3 and H3K27me3 did not cross-react with other trimethylated histone sites, including those highly similar off-targets (Fig. 2*B* and *SI Appendix*, Figs. S1*A* and S3 *A* and *B*). By contrast, many commercially available anti-H3K9me3 antibodies showed cross-reactivity with H3K27me3 (or vice versa) because of a high level of sequence similarity surrounding the modification sites (AR-K9me3-ST versus AR-K27me3-SA) (9, 12). In addition, 2D2-H3, the heterodimeric clasping antibody to H3K9me3, showed better affinity to the target while maintaining high specificity (Fig. 2*B*) compared with the previous homodimeric clasping antibody, 309M3-B (21). A comparison in the peptide IP assay revealed that our clasping antibodies exhibit superior binding

affinity and specificity to the commercial recombinant antibodies we tested (Fig. 2*B* and *SI Appendix*, Fig. S4*A*). Together, these data clearly demonstrate that our new method utilizing yeast display facilitated the identification of high-performance heterodimeric clasping antibodies.

Performance Comparison of an Anti-H3K27me3 Clasping Antibody against a Widely Used Antibody. To test the performance of our clasping antibodies, we chose anti-H3K27me3 clasping antibodies, produced the PTM and enhancer units separately in the Fab format (*SI Appendix*, Fig. S4 *B* and *C*), and coimmobilized them on beads as in Fig. 1*C*. As expected, the coimmobilized Fabs showed high specificity and affinity in the peptide IP assay, consistent with their binding profiles observed in the yeast-display format (Fig. 2*B* and *SI Appendix*, Figs. S3*B* and S4*D*).

We then tested the best clone, 3C2-H2, in Internal Standard Calibrated chromatin immunoprecipitation (ICeChIP) (*SI Appendix*, Fig. S5 *A* and *B*) (33, 34), and a widely used commercial anti-H3K27me3 monoclonal antibody, C36B11, for a side-by-side comparison. ICeChIP utilizes semisynthetic nucleosomes harboring PTMs of interest with barcoded DNAs, allowing for quantitative evaluation of antibody specificity using native-like antigens in the ChIP format. 3C2-H2 specifically captured nucleosomes harboring H3K27me3, and the specificity of 3C2-H2 over other histone modifications was uniformly better than the C36B11 antibody (Fig. 2*C*). Interestingly, 3C2-H2 enriched both asymmetric and symmetric nucleosomes harboring one and two H3K27me3 marks in an unbiased manner, whereas the C36B11 antibody preferentially enriched symmetric nucleosomes (Fig. 2*C*). The bias observed in C36B11 is likely due to the avidity effect resulting from the 2:2 binding stoichiometry between two identical binding sites in C36B11 IgG and two H3K27me3 marks present in a single symmetric nucleosome. Higher enrichment of the symmetric nucleosome harboring both H3K4me3 and H3K27me3 by C36B11 may be a result of both the avidity effect and cross-reactivity (Fig. 2*C*). The clasping antibody, on the other hand, does not have similar avidity effect, because it has 2:1 binding stoichiometry between two Fabs (PTM and enhancer Fabs) and one H3K27me3 mark, rather than the 2:2 stoichiometry. The minimal avidity effect of the clasping antibody is also apparent from the scatter plot of IP versus input reads of nucleosome standards captured by 3C2-H2, in which the fitted lines from linear regression analysis are essentially overlapping for all nucleosomes harboring H3K27me3 tested (*SI Appendix*, Fig. S5*C*). The apparent histone modification density (HMD) peaks contoured over representative loci are similar between 3C2-H2 and C36B11 (Fig. 2 *D* and *E* and *SI Appendix*, Fig. S5*D*). However, the apparent inflation of HMD values was observed using C36B11, likely due to avidity bias for capturing symmetric H3K27me3 nucleosomes of the sort suggested by Voigt et al. (35).

Some of us have revealed as high as a sixfold enrichment difference in ICeChIP for symmetric versus asymmetric nucleosome standards, depending on the mark and the antibody (13, 33). This difference is likely a result of the avidity effect coming from the two binding sites residing in IgG. Given that the H3K27me2/me3 mark is estimated to be ~60% symmetric: ~40% asymmetric in its nucleosome distribution in mouse embryonic stem cells (mESCs) using the standard IgG reagent (35), our clasping antibodies that can capture H3K27me3 evenly may provide a more accurate quantitative measurement of symmetric and asymmetric nucleosomes. Such applications are subjects of future studies. Taken together, our clasping antibody exhibited superior specificity and captured nucleosomes in a less biased manner compared to the available antibody commonly used in the community.

Production of Heterodimeric Clasping Antibodies in an IgG-Like Format. To make clasping antibodies interchangeable with standard antibodies and thus readily usable as research reagents, we next converted anti-H3K27me3 clasping antibodies to the long-neck scFv-Fc antibody format where the PTM and enhancer scFvs are connected to mouse Fc with a long linker to facilitate antigen clasping within a single molecule (21). We introduced the knob-into-hole mutations into the CH3 domain to promote the heterodimer formation (Fig. 3*A*) (36). In addition, a His_6 tag was attached to the C terminus of hole-Fc but not to knob-Fc, facilitating purification of the heterodimer. We also designed an isotype long-neck scFv-Fc as a negative control, where the enhancer unit is replaced with an isotype antibody, while the PTM unit was unchanged. As expected, anti-H3K27me3 clasping antibodies in the long-neck scFv-Fc format exhibited exquisite specificity and high affinity, consistent with the binding profiles of those in the yeast-display and Fab formats, indicating successful production of heterodimeric long-neck scFv-Fc with antigen clasping capability (Fig. 3*B* and *SI Appendix*, Fig. S6 *A* and *B*). Importantly, the isotype long-neck scFv-Fc, composing 4-5 and the nonbinding antibody, showed no detectable binding to any target tested (Fig. 3*B*), further highlighting the potency of antigen clasping. Phosphorylation of the H3K27me3 peptide at S28 moderately reduced the affinity of clasping antibodies by 7 to 20-fold, suggesting that the S28 residue is involved in their antigen recognition and providing additional support for the clasping mechanism (*SI Appendix*, Fig. S6*C*). Biolayer interferometry (BLI) measurements revealed a very slow dissociation rate of clasping antibodies (Fig. 3*C*), an important feature for achieving high efficacy in antigen capture.

Validation in Western blot revealed that clasping antibodies specifically recognized the histone H3 protein in the whole-cell lysate (WCL) (Fig. 3*D* and *SI Appendix*, Fig. S6*D*). Notably, the intense band for histone H3 was absent when the cells were treated with an EZH2 methyltransferase inhibitor, GSK126 (Fig. 3*E*), indicating that target recognition depends on methylation at the H3K27 position. Quantitative native ChIP incorporated with synthetic nucleosomes revealed the 3C2-H2 long-neck scFv-Fc specifically captured nucleosomes harboring H3K27me3, and its specificity was greater than the commercial recombinant antibody to H3K27me3 (Fig. 3*F* and *SI Appendix*, Fig. S6*E*). Together, these data demonstrate that clasping antibodies in the long-neck scFv-Fc format worked well in common applications.

Generation of Clasping Antibodies to Phospho-Tyrosine Antigens. Because of the modular architecture of heterodimeric clasping antibodies, one should be able to develop clasping antibodies to a distinct PTM by replacing the PTM unit with another anti-pan-PTM (i.e., sequence-independent) antibody followed by the identification of appropriate enhancer clones (Fig. 1*B*). To test this plug-and-play possibility, we next set out to generate clasping antibodies to phosphorylated tyrosine (pY) antigens, another class of important PTM antigens. We chose a series of peptides harboring the Grb2-binding motif (pYXNX) as model antigens (24) (*SI Appendix*, Fig. S1*A*), and anti-pan-pY antibody, 4G10 (37), as a PTM unit. The 4G10 antibody in the Fab format exhibited excellent PTM recognition, although it showed sub-micromolar affinity and moderate sequence preference (*SI Appendix*, Fig. S7*A*).

Unexpectedly, 4G10 scFv in the yeast-display format did not bind to the phosphorylated peptides, regardless of the variable domain order in scFv (*SI Appendix*, Fig. S7*B*). The yeast cell wall is negatively charged because of the presence of carboxyl, hydroxyl, and phosphoryl groups (38), and thus, we hypothesized that charged phosphorylated peptides may have limited accessibility to the yeast cell surface due to electric repulsion. Indeed, extending the linker between 4G10

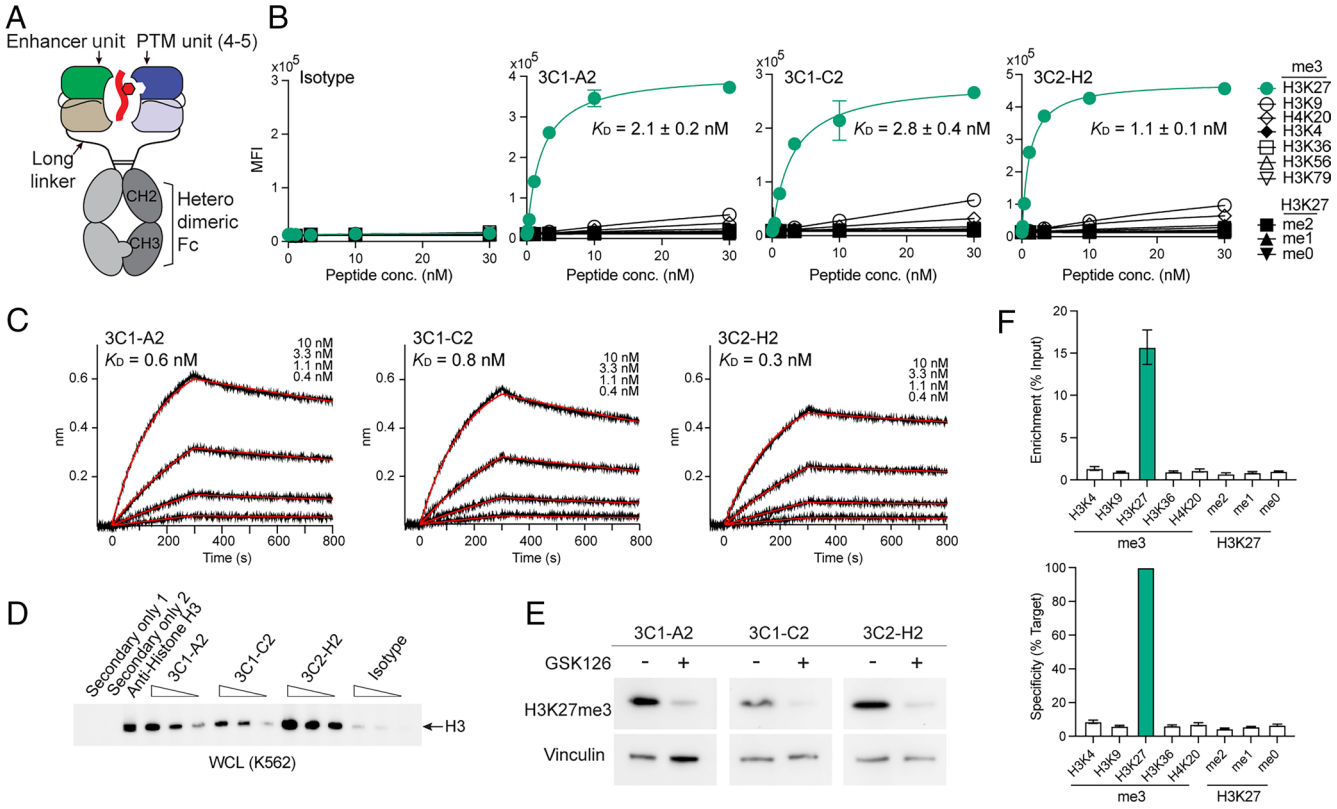

Fig. 3. Characterization of clasping antibodies to H3K27me3 in the long-neck scFv-Fc format. (*A*) Schematic representation of the heterodimeric long-neck scFv-Fc format. Hetero-dimerization is facilitated by the knobs-into-holes mutations in the CH3 domain. (*B*) Binding titration curves of the clasping antibodies against the target and the off-target peptides with the peptide IP assay. The apparent K_D values calculated from the curve fitting of a 1:1 binding model to the target peptide are shown. (*C*) Kinetic analysis of clasping antibodies with BLI. The H3K27me3 peptide was immobilized, and the binding of soluble long-neck scFv-Fc antibodies was measured. The apparent K_D values are from the global fit with a 1:1 binding model to the data. (*D* and *E*) Validation of clasping antibodies in Western blot. (*D*) Whole-cell lysate of K562 cells was blotted with the indicated long-neck scFv-Fc antibodies at three different concentrations (30, 10, and 3.3 nM, respectively). The isotype composes 4-5 (PTM unit) and a nonbinding antibody (in replacement of an enhancer unit) and consequently has weak affinity to Kme3. The "secondary only" lanes refer to no primary antibody with anti-mouse Fc-HRP (secondary only 1) or with anti-rabbit IgG-HRP (secondary only 2). The arrow indicates the location of histone H3. (*E*) Whole-cell lysates from K562 cells treated with and without GSK126, an EZH2 methyltransferase inhibitor, were blotted with indicated long-neck scFv-Fc antibodies. The vinculin protein was detected as a loading control. (*F*) Validation of 3C2-H2 long-neck scFv-Fc in native SNAP-ChIP. The enrichment (percentage of H3K27me3 nucleosome recovered after immunoprecipitation relative to input, *Top*) and specificity (percentage of off-target immunoprecipitation relative to the on-target, *Bottom*) assessed by qPCR are shown. The clasping antibody specifically captured the nucleosome bearing H3K27me3. Data shown in *B* and *F* are from triplicate measurements. Error bars indicate the SD. See *SI Appendix*, Fig. S6 for the complete datasets for Western blot.

scFv and the yeast anchor domain, Aga2 (39), restored the binding of 4G10 to the phosphorylated peptides (*SI Appendix*, Fig. S7*B*), suggesting a successful minimization of the influence of the negatively charged property of the cell surface. We then utilized the longest linker we tested (the CT3 linker) for the yeast-display platform for identifying clasping antibodies for pY antigens.

We next performed phage-display library sorting followed by yeast-display library sorting, essentially the same procedures as for the development of anti-Kme3 clasping antibodies described above. After a few rounds of sorting, we identified clones to the PDGFRb pY716 peptide with single nanomolar apparent K_D values, with weak but detectable binding to an off-target peptide (Fig. 4*A* and *SI Appendix*, Fig. S8 *A–E*). These antibodies in both yeast-display and long-neck scFv-Fc formats showed substantially improved affinity to the intended target peptide compared with the PTM unit alone, supporting their clasping binding mode. Specificity assessment with Western blot using small ubiquitin-like modifier (SUMO)-fusion peptides revealed specific recognition of the PDGFRb pY716 peptide by the clasping antibodies (Fig. 4*B*). The 4G10 antibody in the IgG format detected all phosphorylated SUMO-fusion peptides, despite its low affinity in the monovalent format, likely due to the avidity effect coming from its IgG format (Fig. 4*B*). Indeed, the isotype long-neck scFv-Fc containing a monovalent 4G10 binding unit did not detect any peptides (Fig. 4*B*). The PDG-A5 and PDG-B4 clasping antibodies specifically recognized PDGFRb in a phosphorylation-dependent manner in the WCL (Fig. 4*C* and *SI Appendix*, Fig. S8*F*). Furthermore, the clasping antibodies selectively captured ligand-activated PDGFRb from cell lysate, demonstrating the capability of capturing the intact phosphorylated PDGFRb protein (Fig. 4*D*). Collectively, our platform enabled us to generate clasping antibodies specific to PDGFRb pY716.

We further generated clasping antibodies to the BCR pY177 peptide. The clasping antibodies exhibit high affinity to the BCR pY177 peptide (Fig. 4*E* and *SI Appendix*, Fig. S9 *A–E*), although their specificity is not as optimal as the Kme3 clasping antibodies. In Western blot, the BCR-B8 antibody showed the bands corresponding to BCR-ABL and BCR in the K562 WCL, whereas no band at the corresponding position was observed in the sample treated with phosphatase (Fig. 4*F* and *SI Appendix*, Fig. S9*F*), suggesting selective recognition of phosphorylated BCR. Together, these data suggest the general applicability of our approach to generating high-performance clasping antibodies to site-specific PTMs.

Discussion

In this study, we developed a platform that effectively generates high-performance antibodies to site-specific PTMs. Our platform is built based on a mechanistic understanding of antigen clasping and produces heterodimeric clasping antibodies. An examination

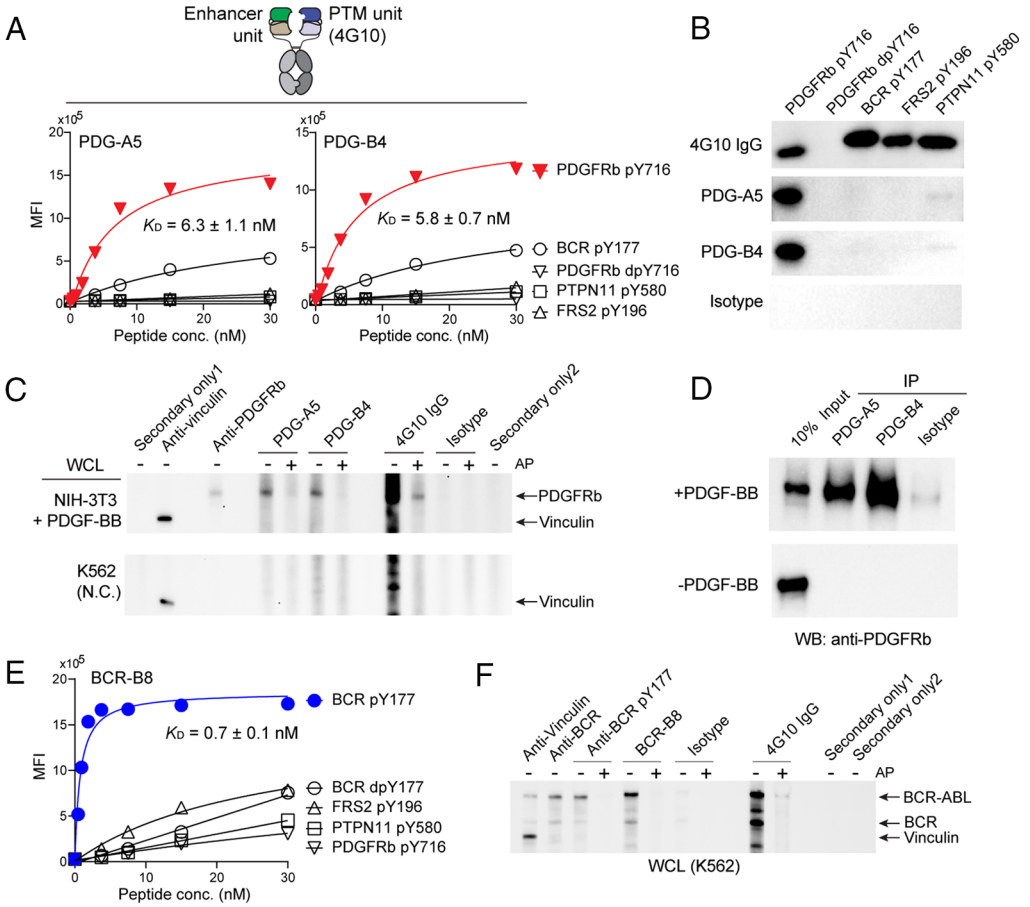

Fig. 4. Characterization of anti-pY clasping antibodies (*A–D*) Characterization of clasping antibodies targeting PDGFRb pY716 in the long-neck scFv-Fc format. (*A*) Binding titration curves of the clasping antibodies with the peptide IP assay. (*B* and *C*) Validation of clasping antibodies in Western blot. SUMO-fused peptides (*B*) and WCLs from platelet-derived growth factor (PDGF)-BB-treated NIH 3T3 cells (*C*, *Top* blot) and K562 cells that do not or minimally express PDGFRb (*C*, *Bottom* blot) were blotted with indicated clasping antibodies and control IgGs. (*D*) Validation of clasping antibodies in IP-Western. The lysates from NIH 3T3 cells treated with or without PDGF-BB were immunoprecipitated with the indicated clasping antibodies, and the immunoprecipitated samples were subsequently blotted with anti-PDGFRb antibody. The clasping antibodies specifically detected and captured PDGFRb in a phosphorylation-dependent manner. (*E* and *F*) Characterization of clasping antibodies targeting BCR pY177 in the long-neck scFv-Fc format with the peptide IP assay (*E*) and Western blot using WCL (*F*). The isotype, used in *B–D* and *F*, composes 4G10 (PTM unit) and a nonbinding antibody (in place of an enhancer unit) and consequently has weak affinity to pY. The apparent K_D values, calculated from the curve fitting of a 1:1 binding model to the target peptide, are shown in *A* and *E*. The abbreviation "dpY" stands for dephosphorylated tyrosine, indicating that the phosphorylation of pY peptides was removed prior to the experiments. The abbreviation "AP" in Western blot (*C* and *F*) stands for alkaline phosphatase and each lane displaying "+" was treated with AP prior to being blotted with antibodies. The "secondary only" lanes refer to no primary antibody with anti-mouse Fc-HRP (secondary only 1) or with anti-rabbit IgG-HRP (secondary only 2). See *SI Appendix*, Figs. S8 and S9 for the complete datasets for Western blot.

of this platform using a series of histone trimethylated peptides resulted in the successful generation of clasping antibodies to H3K9me3, H3K27me3, H3K56me3, and H4K20me3 without iterative optimization. By contrast, our previous attempts by directed evolution without the use of structure information only yielded antibodies to H3K4me3 and H3K9me3 even after extensive efforts (12, 21). Performance comparisons revealed superior specificity and/or affinity of heterodimeric clasping antibodies to existing antibodies, including commercial recombinant antibodies, a current gold standard antibody in the community, and our previous homodimeric clasping antibody. Furthermore, our platform enabled us to generate the clasping antibodies specific to PDGFRb pY716, a target for which the previous attempt did not yield a pY-clamp (24). Collectively, these results demonstrate the effectiveness of our platform.

This study further highlights the potency of the clasping binding mode to achieve high affinity and specificity toward PTMs located within specific sequences. The heterodimeric clasping antibodies in this study showed over 1,000-fold affinity enhancement when targeting histone trimethylated peptides over the affinity of the anti-PTM unit alone. A similar improvement was observed during the development of previous homodimeric clasping antibodies and affinity clamps to the peptides bearing PTMs (21, 24). These observations confirm that this binding mode is optimal for recognizing small-sized antigens, including peptides, PTMs, and small compounds. Achieving such a significant affinity enhancement to those antigens through affinity maturation by solely improving contacts within a single antigen-binding unit, for example, by mutating CDR residues, is challenging, because such conventional approaches are unlikely to result in dramatic increases in the size of the binding interface. We anticipate that our platform can be expanded for developing potent and selective antibodies to many other challenging targets, including intrinsically disordered proteins and small chemical compounds.

The well-established modular structure of antibodies and the plug-and-play feature of heterodimeric clasping antibodies expand the applicability of our platform to essentially any PTMs. We chose the existing anti-pan-PTM antibodies identified through in vitro selection of human naïve library and mouse immunization approaches, respectively (12, 37), indicating that these approaches can be used to identify PTM units for other PTMs. The structure-guided design of anti-pan-PTM antibodies is another option to identify PTM units (40). For identifying enhancer units, we utilized the human synthetic

antibody library (41), but any available libraries, such as human, mouse, and rabbit naive antibody libraries, can also be used as an alternative. Thus, the wide availability of the PTM units and antibody libraries further increases the flexibility of our platform.

The pY clasping antibodies identified in this study showed high affinity and specificity, but their performance was not as excellent as the anti-Kme3 clasping antibodies. A potential explanation is that the current design of anti-pY clasping antibodies may not be optimal, because our design based on the structural understanding of homodimeric anti-H3K4me3 and anti-H3K9me3 clasping antibodies may not directly apply to pY-peptides presented by 4G10. Future structural studies of anti-pY clasping antibodies generated in this study will enhance the efficiency of generating clasping antibodies to pY antigens. Another potential explanation is that 4G10 is not as optimal a PTM unit as the 4-5 antibody for anti-Kme3 clasping antibodies. The 4G10 antibody exhibits apparent K_D values in the sub-micromolar range and moderate sequence preference (*SI Appendix*, Fig. S7*A*), whereas the 4-5 antibody exhibits micromolar apparent K_D values and low sequence preference (12). Thus, reducing the affinity and sequence preference of 4G10 may lead to better clasping antibodies for pY antigens.

Koerber et al. reported the development of anti-PTM antibodies by nature-inspired design (40). They first designed phospho-specific antibody scaffolds by creating anion-binding motifs derived from naturally occurring proteins within CDRs, then randomized residues in other CDRs to generate site-specific anti-PTM antibodies. In contrast to our approach, this approach requires iterative optimization steps, and the final antibodies exhibited moderate affinity. However, this work further exemplifies the potency of binding mode-guided design for generating anti-PTM antibodies.

Zhou et al. reported the development of "bispecific antibody traps" which consist of a generic anti-pY antibody and a conditional antibody that binds to the complex of anti-pY antibody and pY-containing protein, conceptionally similar to our approach (42). However, their approach aims to generate binders targeting the pY sites located within a folded region of a protein. By contrast, our approach targets PTMs in disordered regions, as the majority of PTM sites are found in disordered regions (18–20). Specific recognition of PTMs in disordered regions is challenging due to the entropic loss upon binding and fundamental difficulties in recognizing PTMs. The clasping concept dramatically increases the antigen-binding surface, which helps us overcome this fundamental challenge. Nonetheless, it is intriguing that similar but distinct approaches produced antibodies highly specific to PTMs in folded and disordered regions, further confirming the difficulties in producing potent antibodies to site-specific PTMs and the effectiveness of combining mechanism-guided design and combinatorial library sorting.

Our clasping antibodies are recombinant proteins, and thus, this feature can be exploited for developing unique research tools. For instance, the enzymatically cleavable sites can be added to the C-terminus of clasping Fabs, allowing for the gentle elution of captured nucleosomes in ChIP. Minimal denaturation of nucleosomes during an elution step is critical for an effective reChIP (i.e., sequential ChIP) experiment. Another possible application is that the PTM and enhancer units in the scFv format can be fused with fluorescent proteins and express intracellularly, possibly enabling a fluorescence energy transfer-based biosensor exploiting a large conformational change upon antigen clasping, as demonstrated by some of us using affinity clamps (43). These types of engineering are extremely challenging for polyclonal and monoclonal antibodies. We envision that our platform would produce not only high-performance antibody reagents but also unique tools for elucidating disease mechanisms and cellular events.

Materials and Methods

Antibody selection using phage display and yeast display was performed essentially as described previously (12, 21, 44). Antibody production and characterization, including peptide IP assay, Western blot, ChIP, and IP-Western, were performed essentially following the published methods (11–13, 21, 33, 34). Further details of the materials and methods used in this study are described in *SI Appendix*.

Data, Materials, and Software Availability. ChIP-seq data have been deposited in the Gene Expression Omnibus (GEO) database (GSE270275) (45). All other data are included in the article and/or *SI Appendix*.

ACKNOWLEDGMENTS. We thank Dr. Norihisa Yasui for developing the SUMO-fused phospho-Tyr peptides that were reused in this study and Dr. Oliver Hantschel for providing the 4G10 IgG expression vector. We thank the Small Instrument Fleet instrumentation at New York University Langone Health and the University of Chicago Functional Genomics Facilities. This work was supported by NIH grants R21CA246457 (T.H.), T32-HD007009-45 (R.N.S.), R01-GM115945 (A.J.R.), and R35 GM145373 (A.J.R.).

Author affiliations: [a]Laura and Isaac Perlmutter Cancer Center, New York University Langone Health, New York, NY 10016; [b]Pritzker School of Medicine, The University of Chicago, Chicago, IL 60637; [c]Department of Molecular Genetics and Cell Biology, The University of Chicago, Chicago, IL 60637; [d]Department of Medicine, New York University Grossman School of Medicine, New York, NY 10016; [e]Department of Biochemistry and Molecular Biology, The University of Chicago, Chicago, IL 60637; and [f]Department of Biochemistry and Molecular Pharmacology, New York University Grossman School of Medicine, New York, NY 10016

Author contributions: M.R., R.N.S., A.J.R., S.K., and T.H. designed research; M.R., R.N.S., A.K., and T.H. performed research; M.R. and T.H. contributed new reagents/analytic tools; M.R., R.N.S., A.K., A.J.R., S.K., and T.H. analyzed data; and M.R., R.N.S., A.J.R., S.K., and T.H. wrote the paper.

Competing interest statement: A.J.R. holds equity in EpiCypher. A.K., S.K., and T.H. are listed as inventors of a pending patent on the technology and antibodies developed in this work filed by New York University. A.K., S.K., and T.H. are inventors of US10208110B2 on recombinant histone PTM antibodies managed by the University of Chicago. A.J.R. is a co-inventor of the ICeChIP technology US10732185B2 managed by the University of Chicago and licensed to EpiCypher. A.J.R. is a scientific advisor at EpiCypher. R.N.S. has received consulting fees from EpiCypher. S.K. is a co-founder, receives consulting fees and holds equity in Aethon Therapeutics; is a co-founder and holds equity in Revalia Bio; has received research funding from Aethon Therapeutics, Argenx BVBA, Black Diamond Therapeutics, and Puretech Health, all outside of the current work.

1. B. D. Strahl, C. D. Allis, The language of covalent histone modifications. *Nature* **403**, 41–45 (2000).
2. J. V. Olsen *et al.*, Global, in vivo, and site-specific phosphorylation dynamics in signaling networks. *Cell* **127**, 635–648 (2006).
3. M. Hochstrasser, Ubiquitin-dependent protein degradation. *Annu. Rev. Genet.* **30**, 405–439 (1996).
4. K. Ohtsubo, J. D. Marth, Glycosylation in cellular mechanisms of health and disease. *Cell* **126**, 855–867 (2006).
5. E. L. Greer, Y. Shi, Histone methylation: A dynamic mark in health, disease and inheritance. *Nat. Rev. Genet.* **13**, 343–357 (2012).
6. P. Filippakopoulos, S. Knapp, Targeting bromodomains: Epigenetic readers of lysine acetylation. *Nat. Rev. Drug. Discov.* **13**, 337–356 (2014).
7. T. Pawson, J. D. Scott, Protein phosphorylation in signaling–50 years and counting. *Trends Biochem. Sci.* **30**, 286–290 (2005).
8. S. S. Pinho, C. A. Reis, Glycosylation in cancer: Mechanisms and clinical implications. *Nat. Rev. Cancer* **15**, 540–555 (2015).
9. T. A. Egelhofer *et al.*, An assessment of histone-modification antibody quality. *Nat. Struct. Mol. Biol.* **18**, 91–93 (2011).
10. J. Bordeaux *et al.*, Antibody validation. *Biotechniques* **48**, 197–209 (2010).
11. S. Nishikori *et al.*, Broad ranges of affinity and specificity of anti-histone antibodies revealed by a quantitative peptide immunoprecipitation assay. *J. Mol. Biol.* **424**, 391–399 (2012).
12. T. Hattori *et al.*, Recombinant antibodies to histone post-translational modifications. *Nat. Methods* **10**, 992–995 (2013).
13. R. N. Shah *et al.*, Examining the roles of H3K4 methylation states with systematically characterized antibodies. *Mol. Cell* **72**, 162–177.e7 (2018).
14. G. Kohler, C. Milstein, Continuous cultures of fused cells secreting antibody of predefined specificity. *Nature* **256**, 495–497 (1975).
15. A. R. M. Bradbury *et al.*, When monoclonal antibodies are not monospecific: Hybridomas frequently express additional functional variable regions. *MAbs* **10**, 539–546 (2018).
16. J. Voskuil, Commercial antibodies and their validation. *F1000Res.* **3**, 232 (2014).

17. A. Bradbury, A. Pluckthun, Reproducibility: Standardize antibodies used in research. *Nature* **518**, 27–29 (2015).
18. C. N. Pang, A. Hayen, M. R. Wilkins, Surface accessibility of protein post-translational modifications. *J. Proteome Res.* **6**, 1833–1845 (2007).
19. V. Pejaver *et al.*, The structural and functional signatures of proteins that undergo multiple events of post-translational modification. *Protein Sci.* **23**, 1077–1093 (2014).
20. M. Narasumani, P. M. Harrison, Discerning evolutionary trends in post-translational modification and the effect of intrinsic disorder: Analysis of methylation, acetylation and ubiquitination sites in human proteins. *PLoS Comput. Biol.* **14**, e1006349 (2018).
21. T. Hattori *et al.*, Antigen clasping by two antigen-binding sites of an exceptionally specific antibody for histone methylation. *Proc. Natl. Acad. Sci. U.S.A.* **113**, 2092–2097 (2016).
22. J. Huang, A. Koide, K. Makabe, S. Koide, Design of protein function leaps by directed domain interface evolution. *Proc. Natl. Acad. Sci. U.S.A.* **105**, 6578–6583 (2008).
23. S. Koide, J. Huang, Generation of high-performance binding proteins for peptide motifs by affinity clamping. *Methods Enzymol.* **523**, 285–302 (2013).
24. N. Yasui *et al.*, Directed network wiring identifies a key protein interaction in embryonic stem cell differentiation. *Mol. Cell* **54**, 1034–1041 (2014).
25. U. Brinkmann, R. E. Kontermann, The making of bispecific antibodies. *MAbs* **9**, 182–212 (2017).
26. T. Kouzarides, Chromatin modifications and their function. *Cell* **128**, 693–705 (2007).
27. A. Barski *et al.*, High-resolution profiling of histone methylations in the human genome. *Cell* **129**, 823–837 (2007).
28. L. Cai, X. Ma, Y. Huang, Y. Zou, X. Chen, Aberrant histone methylation and the effect of Suv39H1 siRNA on gastric carcinoma. *Oncol. Rep.* **31**, 2593–2600 (2014).
29. K. H. Kim, C. W. Roberts, Targeting EZH2 in cancer. *Nat. Med.* **22**, 128–134 (2016).
30. M. F. Fraga *et al.*, Loss of acetylation at Lys16 and trimethylation at Lys20 of histone H4 is a common hallmark of human cancer. *Nat. Genet.* **37**, 391–400 (2005).
31. D. Husmann, O. Gozani, Histone lysine methyltransferases in biology and disease. *Nat. Struct. Mol. Biol.* **26**, 880–889 (2019).
32. S. Zhao, C. D. Allis, G. G. Wang, The language of chromatin modification in human cancers. *Nat. Rev. Cancer* **21**, 413–430 (2021).
33. A. T. Grzybowski, Z. Chen, A. J. Ruthenburg, Calibrating ChIP-Seq with nucleosomal internal standards to measure histone modification density genome wide. *Mol. Cell* **58**, 886–899 (2015).
34. A. T. Grzybowski, R. N. Shah, W. F. Richter, A. J. Ruthenburg, Native internally calibrated chromatin immunoprecipitation for quantitative studies of histone post-translational modifications. *Nat. Protoc.* **14**, 3275–3302 (2019).
35. P. Voigt *et al.*, Asymmetrically modified nucleosomes. *Cell* **151**, 181–193 (2012).
36. J. B. Ridgway, L. G. Presta, P. Carter, "Knobs-into-holes" engineering of antibody CH3 domains for heavy chain heterodimerization. *Protein Eng.* **9**, 617–621 (1996).
37. B. J. Druker, H. J. Mamon, T. M. Roberts, Oncogenes, growth factors, and signal transduction. *N. Engl. J. Med.* **321**, 1383–1391 (1989).
38. J. S. White, G. M. Walker, Influence of cell surface characteristics on adhesion of Saccharomyces cerevisiae to the biomaterial hydroxylapatite. *Antonie Van Leeuwenhoek* **99**, 201–209 (2011).
39. P. S. Lown *et al.*, Extended yeast surface display linkers enhance the enrichment of ligands in direct mammalian cell selections. *Protein Eng. Des. Sel.* **34**, gzab004 (2021).
40. J. T. Koerber, N. D. Thomsen, B. T. Hannigan, W. F. Degrado, J. A. Wells, Nature-inspired design of motif-specific antibody scaffolds. *Nat. Biotechnol.* **31**, 916–921 (2013).
41. F. A. Fellouse *et al.*, High-throughput generation of synthetic antibodies from highly functional minimalist phage-displayed libraries. *J. Mol. Biol.* **373**, 924–940 (2007).
42. X. X. Zhou *et al.*, Targeting phosphotyrosine in native proteins with conditional, bispecific antibody traps. *J. Am. Chem. Soc.* **142**, 17703–17713 (2020).
43. J. Huang, S. Koide, Rational conversion of affinity reagents into label-free sensors for Peptide motifs by designed allostery. *ACS Chem. Biol.* **5**, 273–277 (2010).
44. K. R. Miller *et al.*, T cell receptor-like recognition of tumor in vivo by synthetic antibody fragment. *PLoS One* **7**, e43746 (2012).
45. M. Riso *et al.*, Structure-guided development of high-performance antibodies targeting site-specific post-translational modifications. Gene Expression Omnibus (GEO). https://www.ncbi.nlm.nih.gov/geo/query/acc.cgi?acc=GSE270275. Deposited 20 June 2024.